arXiv:nucl-th/0601013v2 29 Sep 2006

A critical view on the deeply bound K^-pp system

V.K. Magas[1], E. Oset[2], A. Ramos[1] and H. Toki[3]
[1] *Departament d'Estructura i Constituents de la Matèria, Universitat de Barcelona, Diagonal 647, 08028 Barcelona, Spain*
[2] *Departamento de Física Teórica and IFIC Centro Mixto Universidad de Valencia-CSIC, Institutos de Investigación de Paterna Apdo. correos 22085, 46071, Valencia, Spain and*
[3] *Research Center for Nuclear Physics, Osaka University, Ibaraki, Osaka 567-0047, Japan*
(Dated: November 18, 2013)

We briefly review the situation around the claimed deeply bound K^- states in different recent experiments and concentrate particularly on the state K^-pp advocated by the FINUDA collaboration in nuclear K^- absorption. We perform a theoretical simulation of the process and show that the peak in the Λp spectrum that was interpreted as a deep K^-pp bound state corresponds mostly to the process $K^-pp \to \Lambda p$ followed by final state interactions of the produced particles with the daughter nucleus.

PACS numbers: 13.75.-n; 13.75.Jz; 21.65.+f; 25.80.Nv

I. INTRODUCTION

The theoretical predictions of deeply bound pionic atoms [1, 2, 3, 4], which were observed in the $(d,\ ^3\mathrm{He})$ reaction [5, 6], following a suggestion of the theoretical studies of [7, 8], have stimulated the search for bound states of different hadrons in nuclei. One of the natural continuations was the study of K^- bound states. The large potential used at that time [9] to reproduce existing data on K^- atoms fed the ideas that deeply bound K^- states (bound by $50-200$ MeV) could exist. The question, of course, arises, as to whether the widths of the states are narrow enough to distinguish between neighboring states. One should distinguish these deeply bound states from other states bound by a few MeV in heavy nuclei that different realistic potentials predict and which have not yet been observed [10, 11, 12, 13].

A step forward in the theoretical description of the K^- nucleus optical potential was given in [14] establishing a link between the optical potential and the presence of the $\Lambda(1405)$ resonance, which, in free space, appears 27 MeV below the K^-p threshold. In the medium, the effect of Pauli blocking on the excitation of intermediate $\bar{K}N$ states demanded more energy to have the same phase space, as a consequence of which the $\Lambda(1405)$ was produced at higher energies. Correspondingly, the zero in the real part of the in-medium K^-p amplitude appears above the K^-p threshold and, as a consequence, the repulsive free-space K^-p amplitude at threshold turns into an attractive one in the medium.

The effect described above remains in all present theoretical works as the driving mechanism to get an attractive K^- nucleus optical potential. Yet, the fact that the K^- feels an attractive self-energy in the medium facilitates the generation of the $\Lambda(1405)$ at smaller energies, moving the zero of the amplitude back to smaller energies and, eventually, ending up below the K^-N threshold leading again to repulsion. It becomes clear at this point that a self-consistent calculation is needed, and it was done in [15] where a small attraction was finally found with the resonance position barely modified.

Subsequent improvements introducing also the self-energy of the pions and the baryons were done in [16] by means of which a potential was obtained that reproduced the data for the K^- atoms [12]. This potential, which automatically accounts for new many body decay channels with respect to former ones, like $K^-NN \to \Sigma N,\ \Lambda N,\ \Sigma^* N$, leads to deeply bound states with $B \approx 30$ MeV, but the width of the states is around 100 MeV [12]. Potentials with the same strength when self-consistency is imposed are found in [16, 17, 18].

With this behavior for the $\bar{K}N$ dynamics in nuclei having been established, the claim given in [19] on the possible existence of narrow deeply bound states in $A = 3, 4$ nuclei, predicting a $A = 3,\ I = 0$ state with a binding energy of 100 MeV, was surprising. The situation became more puzzling when an experiment searching for deeply bound K^- states using the reaction ^{4}He(stopped K^-, p) [20] found a signal for a strange tri-baryon, $S^0(3115)$, which was claimed not to correspond to the state predicted in [19], since its interpretation as a bound state would imply a binding energy around 200 MeV and the state had $I = 1$. Subsequent corrections of the potential in [21] involving some spin-orbit effects and relativistic corrections (which had been accounted for in other works [16, 17]), plus some extra ad hoc modifications, could lead to the extra binding of the kaon, as a consequence of which the findings of [20] have been lately presented as evidence of deeply bound K^- atoms [22, 23].

In a recent paper [24] two of us make a critical review of the theoretical works [19, 21] and also of the interpretation of the peak in the experiment of [20]. The main criticisms raised in [24] are the following. The theoretical potential in [19, 21] eliminates the direct coupling of $\pi\Sigma \to \pi\Sigma$ and $\pi\Lambda \to \pi\Lambda$ in contradiction with the results of chiral theory that establishes large couplings for them

[25]. This assumption prevents the finding of two $\Lambda(1405)$ states as appears recently in all chiral unitary approaches for the $\bar{K}N$ system [26, 27, 28, 29, 30] and which gets experimental support from the study of the $K^-p \to \pi^0\pi^0\Sigma^0$ reaction [31] done in [32]. The experimental $\Lambda(1405)$ resonance, which is a superposition of these two states, is assumed in [19, 21] to be a bound state of $\bar{K}N$, contradicting the results of the chiral theories and leading to a $\bar{K}N$ amplitude in $I = 0$ twice as large below the K^-p threshold. The self-consistency shown to be essential in [15, 16, 17] is not implemented in [19, 21] and, finally, the system is allowed to shrink to densities as large as 10 normal nuclear densities, $\rho = 10\rho_0$, at the center of the nucleus resulting into a deeper K^- nucleus potential. With all these assumptions and approximations, the potential of [21] has a strength of about a factor twenty larger than that of the chiral approach. Furthermore, the work of [19, 21] does not take into account the many body decay channels considered in [16] and, as was shown in [24], had they been included, and with the densities claimed in [19, 21], the width of the K^- state should have been of the order of 200 MeV or higher, instead of the width of about 20 MeV assumed in [19, 21].

Convinced by these arguments that the peak found at KEK [20] could not correspond to a deeply bound K^- state, the authors of [24] searched for other explanations and found a natural mechanism that passed all tests. The peak is due to the reaction $K^-NN \to \Sigma p$ in ^{4}He leaving the other nucleons as spectators. Such an interpretation demanded the peak corresponding to the reaction $K^-NN \to \Lambda p$ be seen as well, which was indeed the case in the experiment. This latter peak disappeared when a cut for "fast" pions was done (the pions coming from Λ decay have momentum in the range $61 - 196$ MeV/c) and was prominent in the complementary cut of "slow pions". The interpretation demanded that the peaks had to be seen in other nuclei, a test also passed by the FINUDA data on the proton spectrum presented in [33]. In addition, the requirement that the daughter nucleus is just a spectator becomes more difficult in heavier nuclei since the distortion of the Λ or p particle in their way out through the nucleus leads unavoidably to nuclear excitations. As a consequence of this, one expects the signals to fade gradually for heavier nuclei, which is also a feature of the FINUDA data on the proton spectrum.

With the situation of the KEK experiment clarified, the reanalysis of the interpretation of the FINUDA data on the Λp invariant mass, leading to a claim of a bound state of K^-pp by 115 MeV, is an absolute necessity and this is the purpose of the present work.

The FINUDA collaboration in [34] looks for Λp events back to back following the K^-pp absorption in ^{6}Li, ^{7}Li and ^{12}C nuclei. A narrow peak in the invariant mass is observed, which is identified with $K^-pp \to \Lambda p$ removing just the binding energy. This implicitly assumes ground state formation of the daughter nucleus since nuclear excitations lead necessarily to a broad peak, namely the quasielastic peak. On the other hand, a broad second peak of about 60 MeV width, which is identified in [34] as a signal for the K^-pp bound state, is seen at smaller Λp invariant masses and of much larger strength than the first peak. In the present work we shall see that this peak, with its strength, position, width and angular dependence corresponds to the same two-nucleon absorption mechanism discussed above, but leading to nuclear excitation, which has a much larger strength than the fraction leading to the ground state in the daughter nucleus.

To reach the former conclusion, a computer simulation calculation is made allowing the stopped kaons in the nucleus to be absorbed by a pair of nucleons of a local Fermi sea. The nucleon and the Λ emitted in the $K^-pp \to \Lambda p$ and $K^-pn \to \Lambda n$ absorption processes are allowed to re-scatter with other nucleons in the nucleus leading to nuclear breakup and producing a nucleon spectrum with a distinct peak corresponding to one collision. This peak, which is analogous to the quasielastic peak of any inclusive reaction like (e, e'), (π, π'), (p, p') etc, reproduces the experimental peak taken in [34] as a signal of the K^-pp bound state. Another peak, broader and at smaller energies coming from baryon secondary collisions, also appears both in our simulation and in the experimental data at the same place and hence, an explanation for the whole experimental spectrum is found, which does not require to invoke the creation of the K^-pp bound state.

II. THE THEORETICAL FRAMEWORK

The results of [34] are presented for a mixture of data from ^{6}Li, ^{7}Li and ^{12}C. We shall perform our calculations for these nuclei, as well as for the other two targets installed in the FINUDA apparatus, ^{27}Al and ^{51}V, although the invariant mass spectrum was only shown for the three lighter nuclei. The reaction is

$$K^- \; A \to \Lambda \; p \; A' \tag{1}$$

with stopped kaons. The Λp events are collected and, as done in the experiment, two cuts are made: one selecting $p_\Lambda > 300$ MeV/c, to eliminate events from $K^-p \to \Lambda\pi$, and another one imposing $\cos\Theta_{\vec{p}_\Lambda \vec{p}_p} < -0.8$, to filter Λp pairs going back to back.

The K^- absorption at rest proceeds by capturing a slow K^- in a high atomic orbit of the nucleus, which later cascades down till the K^- reaches a low lying orbit, from where it is finally absorbed by the nucleus. According to Refs. [35, 36] from a study of the cascade of electromagnetic (EM) transitions after trapping slow pions in nuclei, the nuclear absorption takes place from the lowest atomic orbit and the next higher one where one has data for the atomic energy shifts. This is so since, as soon as the absorption takes place, it overcomes the EM transition precluding the observation of the X rays. Application of the cascade absorption rates to radiative pion

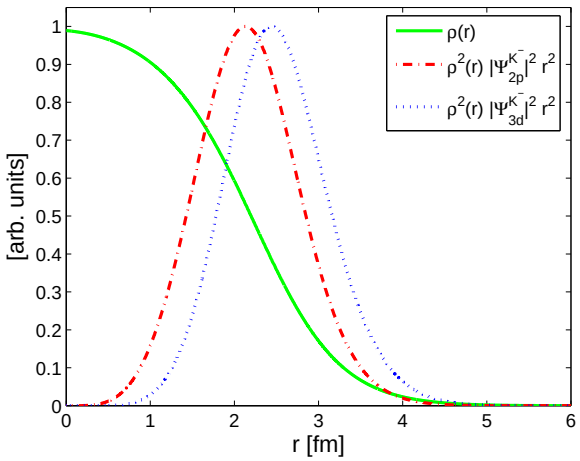

FIG. 1: (Color online) Nuclear density profile for ^{12}C (solid line) and overlap $|\Psi_{K^-}(\vec{r})|^2 r^2 \rho^2(r)$ for a $2p$ (dot-dashed line) or $3d$ (dotted line) kaonic atom states.

capture has been done with success in [37, 38]. The rational of the absorption probability from the (n, l) levels is the same for kaonic atoms and, hence, we also assume the absorption to take place from the lowest level where the energy shift for atoms has been measured, or, if it is not measured, from the level where the calculated shift [12] falls within the measurable range. In the case of ^{6}Li, ^{7}Li, ^{12}C, ^{27}Al and ^{51}V, the absorption takes place from the orbits $2p$, $2p$, $2p$, $3d$ and $4f$ respectively. We will also explore how the invariant Λp mass spectrum changes in ^{12}C when the K^- is assumed to be absorbed from the higher $3d$ orbit.

The cut $p_\Lambda > 300$ MeV/c in the experiment allows us to neglect the one body $K^- N \to \Lambda\pi$ reaction and concentrate exclusively on the two body absorption mechanism. In Fig. 1 we represent the density profile for ^{12}C (solid line), together with the quantity $|\Psi_{K^-}(r)|^2 r^2 \rho^2(r)$, which represents an overlap function for the K^- being absorbed by a pair of nucleons. The dot-dashed line represents the overlap when the K^- is absorbed from an atomic $2p$ orbit, whereas the dotted line represents the absorption from a $3d$ state. Both overlap functions have been scaled such that their maximum value is 1, but we note that the overlap for the $3d$ orbit is in fact 4 orders of magnitude smaller than that for the $2p$ one. However, this small magnitude does not mean that the absorption rate from that state is so much smaller than that from the $2p$ state since in the latter case one must also take into account the EM transition probability from the $3d$ to $2p$ state in the cascade process [35, 36]. This is why we also calculate the Λp invariant mass distribution following absorption from the $3d$ state.

The K^- absorption width from pN pairs in a nucleus with A nucleons is proportional in first approximation to the square of the nuclear density [39] multiplied by the probability of finding the K^- in the nucleus, hence, it is given by the expression:

$$\Gamma_A = \text{Norm} \int d^3\vec{r} |\Psi_{K^-}(\vec{r})|^2 \left(\frac{\rho(r)}{2}\right)^2 \Gamma_m =$$
$$= \text{Norm} \int d^3\vec{r} |\Psi_{K^-}(\vec{r})|^2 \;\; 2 \int \frac{d^3\vec{p}_1}{(2\pi)^3} \Theta(k_F(r) - |\vec{p}_1|)$$
$$\times \; 2 \int \frac{d^3\vec{p}_2}{(2\pi)^3} \Theta(k_F(r) - |\vec{p}_2|) \;\; \Gamma_m(\vec{p}_1, \vec{p}_2, \vec{p}_K, \vec{r}) \;, \quad (2)$$

where we have used $\rho(r) = 4 \int \frac{d^3\vec{p}_1}{(2\pi)^3} \Theta(k_F(r) - |\vec{p}_1|)$ for the nucleons with momenta $\vec{p}_1$, $\vec{p}_2$ in the Fermi sea, k_F is the Fermi momentum at the local point, Θ is the step function, Norm is a proportionality constant that has dimensions of R^6 and $\Gamma_m(\vec{p}_1, \vec{p}_2, \vec{p}_K, \vec{r})$ is the in-medium decay width for the $K^- pN \to \Lambda N$ process given by

$$\Gamma_m(\vec{p}_1, \vec{p}_2, \vec{p}_K, \vec{r}) = \int \frac{d^3\vec{p}_\Lambda}{(2\pi)^3} \frac{M_\Lambda}{p^0_\Lambda} \int \frac{d^3\vec{p}_N}{(2\pi)^3} \frac{M_N}{p^0_N} \; (2\pi)^4$$
$$\times \delta^4(p_\Lambda + p_N - p_1 - p_2 - p_K)$$
$$\times \frac{\overline{\sum_{s_i}} \sum_{s_f} |T_{K^- pN \to \Lambda N}|^2}{m_K + p^0_1 + p^0_2} \Theta(|\vec{p}_N| - k_F(r)) \quad (3)$$

where $\vec{p}_K$, $\vec{p}_\Lambda$, $\vec{p}_N$ are momenta of the corresponding particles, and $\frac{\overline{\sum_{s_i}} \sum_{s_f} |T_{K^- pN \to \Lambda N}|^2}{m_K + p^0_1 + p^0_2}$ will be assumed to be approximately constant for $\vec{p}_K = 0$, and $|\vec{p}_1|, |\vec{p}_2| \ll M$.

Now we insert Eq. (3) into Eq. (2), perform the integration over $d^3\vec{p}_1$ and the angular part of $d^3\vec{p}_2$, and absorb all the constants into Norm:

$$\Gamma_A = \text{Norm} \int d^3\vec{r} |\Psi_{K^-}(\vec{r})|^2 \int \frac{d^3\vec{p}_\Lambda}{p^0_\Lambda} \int \frac{d^3\vec{p}_N}{p^0_N}$$
$$\times \int dp_2 p_2 \frac{p^0_\Lambda + p^0_N - p^0_2 - m_K}{|\vec{P}|} \; \Theta(1 - A^2)$$
$$\times \; \Theta\left(k_F(r) - \sqrt{|\vec{P}|^2 + |\vec{p}_2|^2 - 2|\vec{P}||\vec{p}_2|A}\right)$$
$$\times \; \Theta(k_F(r) - |\vec{p}_2|) \Theta(|\vec{p}_N| - k_F(r)) \;, \quad (4)$$

where $\vec{P} = \vec{p}_\Lambda + \vec{p}_N$, and A provides the cosine of the angle between $\vec{P}$ and $\vec{p}_N$,

$$A \equiv \cos\Theta_{\vec{P}\vec{p}_N} \equiv$$
$$\equiv \frac{M_N^2 + \vec{P}^2 + \vec{p}_2^{\,2} - (p^0_\Lambda + p^0_N - p^0_2 - m_K)^2}{2|\vec{P}||\vec{p}_2|} \,. \quad (5)$$

In order to take into account the propagation of the produced nucleon and Λ through the nucleus after K^- absorption we insert a kernel $K(\vec{p}, \vec{r})$ into Eq. (4) for both particles. This kernel has been used in Monte Carlo simulations of pion nucleus reactions [40], proton nucleus reactions [41], electron nucleus reactions [42], leading to good reproduction of inclusive cross sections and selected channels of one and two nucleon emission, etc. Thus the

final expression for the K^- absorption width from pN pairs in nucleus A is given by

$$\Gamma_A = \mathrm{Norm} \int d^3\vec{r}\,|\Psi_{K^-}(\vec{r})|^2 \int \frac{d^3\vec{p}_\Lambda}{p^0_\Lambda} \int \frac{d^3\vec{p}_N}{p^0_N} \times \int dp_2 p_2 \frac{p^0_\Lambda + p^0_N - p^0_2 - m_K}{|\vec{P}|}\ \Theta(1-A^2) \times \Theta\left(k_F(r) - \sqrt{|\vec{P}|^2 + |\vec{p}_2|^2 - 2|\vec{P}||\vec{p}_2|A}\right) \times \Theta(k_F(r) - |\vec{p}_2|)\Theta(|\vec{p}_N| - k_F(r)) \times K(\vec{p}_\Lambda, \vec{r})K(\vec{p}_N, \vec{r})\ . \quad (6)$$

The procedure accomplished by Eq. (6) is the following. A kaon at rest is absorbed from the surface of the nucleus by two nucleons (pp or pn) whose momenta are chosen randomly from the local Fermi sea, with a Fermi momentum $k_F(r) = \left(3\pi^2\rho(r)/2\right)^{1/3}$, where $\rho(r)$ is the experimental nuclear density. Energy and momentum conservation is demanded according to phase space and hence two momenta of the emitted p (n) and Λ are generated. Then, the primary nucleon is allowed to re-scatter with nucleons in the nucleus by means of

$$pN \to p'N' \qquad np \to pn \quad (\text{fast } n \text{ to fast } p) \quad (7)$$

according to a probability per unit length given by $\sigma\rho(r)$, where σ is the experimental NN cross section at the corresponding energy. The Λ is allowed to scatter similarly, assuming a cross section of $\sigma_{\Lambda N} \equiv \frac{2}{3}(\sigma_{pN}+\sigma_{nN})$, which is a reasonable choice based on the observation that realistic YN potentials predict a Λ mean-field potential depth in nuclei of about 2/3 that of the nucleon [43]. The nucleons from the Fermi sea that participate in the collisions are also chosen randomly, the variables of the scattering particles are boosted to their Center of Mass (c.m.) frame, an angular distribution is generated according to experiment (for ΛN it is assumed to be the same as for NN) and a boost back to the Lab frame is performed. After several possible collisions, one or more nucleons and a Λ emerge from the nucleus and the invariant mass of all possible Λp pairs, as well as their relative angle, are evaluated for each Monte Carlo event and stored conveniently to generate the required histograms.

III. FORMATION OF THE GROUND STATE OF THE FINAL DAUGHTER NUCLEUS

Absorption of K^- from a nucleus leaving the final daughter nucleus in its ground state gives rise to a narrow peak in the Λp invariant mass distribution, as it is observed in the spectrum of [34]. Our local density formalism, in which the hole levels in the Fermi sea form a continuum of states, cannot handle properly transitions to discrete states of the daughter nucleus, in particular to the ground state. For this reason, we will remove in our calculations those events in which the p and Λ produced after K^- absorption leave the nucleus without having suffered a secondary collision.

A precise value for the strength going into the ground state of the daughter nucleus would require a quantum mechanical calculation with a good description of the nuclear wave functions. However, for the purpose of finding an interpretation to the second peak of the FINUDA experiment of about 60 MeV wide, this knowledge is not strictly necessary. In this section we give qualitative arguments to estimate the strength of the ground-state to ground-state process, with the only aim of showing that it represents a moderate fraction of the total, meaning that a significant amount of strength will go to nuclear excitations, generating the typical quasiparticle peak which the FINUDA collaboration interprets as a bound K^-pp state. Let's take as an example the case of ^{7}Li. The process under consideration would be

$$K^-\ {}^7\mathrm{Li} \to p\ \Lambda\ {}^5\mathrm{H}\,. \quad (8)$$

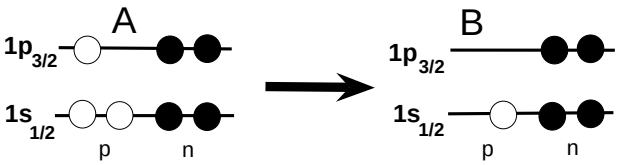

FIG. 2: A) The ground state of ^{7}Li; B) The ground state of ^{5}H.

A simple shell model structure of ^{7}Li is given in Fig. 2A. In the same picture the ground state (g.s.) of the daughter nucleus after the removal of two protons would be given by Fig. 2B. It is clear that even if ^{5}H had an approximate structure like in Fig. 2B, its orbitals are different from those of the ^{7}Li, which means that the overlap of the corresponding wave functions is smaller than 1:

$$| < \Psi_{^5\mathrm{H}}(gs)|\Psi_{^7\mathrm{Li}}(gs)(pp)^{-1} > | < 1\,. \quad (9)$$

Actually, for the discussion that follows, we do not need to know the precise value of this overlap. Values for it of the order of $0.5-0.7$ are already large, which would lead to a formation probability, defined as

$$\text{Form. prob.} = | < \Psi_{^5\mathrm{H}}(gs)|\Psi_{^7\mathrm{Li}}(gs)(pp)^{-1} > |^2\,, \quad (10)$$

of the order or smaller than 0.3. The formation probability is a concept used in α decay, where such an overlap plays an important role in the decay rates when four particles are removed from the father nucleus [44].

The formation probability is not all what matters in the reaction. In α decay one has to consider the probability of penetrating through the potential barrier. In the present case the formation probability has to be weighted

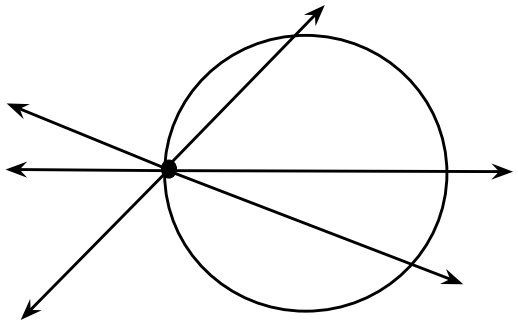

FIG. 3: A simplified K^- absorption picture for the estimation of the survival probability.

by the "survival probability", corresponding to the situation in which both the p and the Λ cross the daughter nucleus without any collision. This is so because any such collision would excite the nucleus, which would then not remain in its ground state. By looking at Fig. 3 one observes that, for the K^- being absorbed on the surface, only one baryon (p or Λ) will cross the nucleus, and the survival probability would be

$$P_s = \mathrm{e}^{-\int_0^\infty \sigma\rho(\vec{r}\,')dl}\,, \tag{11}$$

where $\vec{r}\,' = \vec{r} + l\vec{p}/p$ is the production point and $\sigma \simeq$ 20 mb for 581 MeV/c, corresponding to the momentum of the proton coming from $K^-pp \to p\Lambda$ absorption. A simple estimate using Eq. (11) gives $P_s \simeq 0.4$ for ^{12}C, which is confirmed by the more accurate value extracted from our Monte Carlo simulations, namely $P_s = 0.397$ assuming K^- absorption from the $2p$ orbit and $P_s = 0.396$ for absorption from the $3d$ orbit. In the case of ^{7}Li our Monte Carlo simulation gives a value of $P_s = 0.56$, while for other nuclei we obtain $P_s = 0.59$ in ^{6}Li, $P_s = 0.26$ in ^{27}Al, and $P_s = 0.18$ in ^{51}V. Combining this factor with the formation probability of ≤ 0.3, we finally estimate a probability smaller than about 15% for having the daughter nucleus in its ground state after a K^-pp absorption event. Although crude, the former evaluation of the role of the ground state formation is sufficient for our purposes, since we are only interested in the position and shape of the quasielastic peak, which does not depend on the precise value of the proportion of strength going to the ground state relatively to that going to nuclear excitations.

It should also be mentioned here that the possibility of removing two protons from the s-wave orbit in Fig. 2 leading to a final ^{5}H excited nucleus in the continuum without further interaction of the p or Λ is negligible due to the small overlap between these two states. This means in practice that the excitation of the nucleus will require the secondary collision of the p or Λ after the K^-pp absorption process. This is indeed what happens, for instance, in (p,p') collisions, where the strength of the cross section to elastic or bound excited states is very small compared to that of nuclear breakup producing the quasielastic peak.

In Fig. 3 of Ref. [34] a narrow peak is observed around $\sqrt{s} = 2350$ MeV, already interpreted by the authors as the g.s. formation process described above. If this process accounts for a relatively small fraction of the K^- absorption rate, obviously the bulk of the strength will go into the region of smaller invariant Λp mass. One can then immediately guess that the broad peak to the left of the narrow peak in the spectrum of Fig. 3 of [34] will account for these events. To check this hypothesis we present in the next section the distribution of strength for the events in which the emitted particles following K^- absorption undergo collisions in their way out of the daughter nucleus, after having applied the same cuts in the Λ momentum and the Λp relative angle as in the experiment [34].

IV. SPECTRUM OF THE SECONDARY COLLISIONS

The spectrum of secondary collisions is generated from our computer simulation algorithm of Eq. (6) which allows the particles emitted after K^- absorption to rescatter in their way out of the daughter nucleus. The nucleons move under the influence of a mean field potential which we take to be given by the Thomas-Fermi expression:

$$V(r) = -\frac{k_F(r)^2}{2m_N}\,. \tag{12}$$

For each nucleus under consideration, an extra constant binding Δ is added to the hole nucleon spectrum, such that the maximum ΛN invariant mass allowed by our model, $m_{K^-} + 2M_p - 2\Delta$, corresponds to the actual invariant mass reached in K^- absorption leading to the ground state of the daughter nucleus, $m_{K^-} + M(A,Z) - M(A-2,Z-2)$. Taking the experimental values of the nuclear masses we obtain $\Delta = 15.2$, 16.2, 12.8, 10.7 and 9.6 MeV for ^{6}Li, ^{7}Li, ^{12}C, ^{27}Al and ^{51}V, respectively.

The results of the calculated spectra with just one collision after K^- absorption in ^{12}C are shown in Fig. 4. A momentum cut of $p_\Lambda > 300$ MeV/c has already been imposed since this condition is fulfilled by almost all absorption events. On inspecting the thick line, which corresponds to the sum of the two possible absorption mechanisms, K^-pp and K^-pn, with final state interactions (FSI), one can see a main bump in the spectrum, which peaks around the same position and is somewhat broader than the main peak shown in the insert of Fig. 3 of [34]. Since one measures the Λp invariant mass, the main contribution comes from $K^-pp \to \Lambda p$ absorption. The contribution from the $K^-pn \to \Lambda n$ reaction

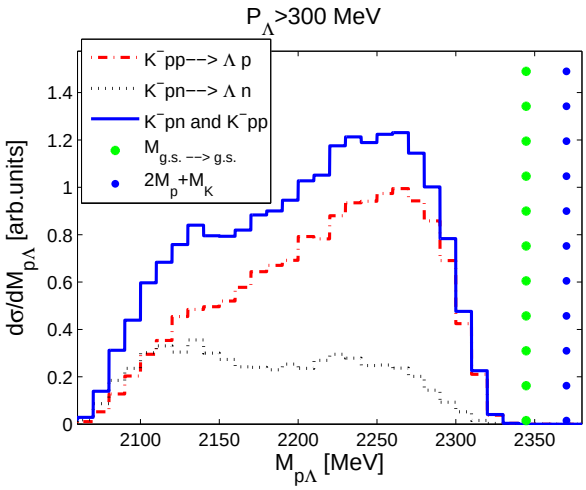

FIG. 4: (Color online) Invariant mass of Λp distribution for K^- absorption in ^{12}C with maximum one collision of the outgoing particles with the daughter nucleus.

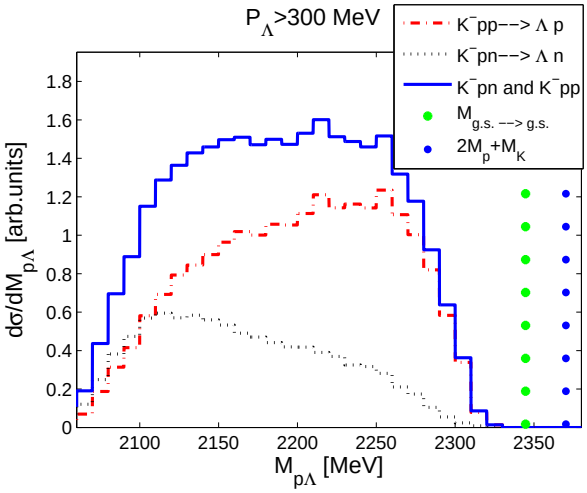

FIG. 6: (Color online) Invariant mass of Λp distribution for K^- absorption in ^{12}C allowing up to three collisions of the outgoing particles with the daughter nucleus.

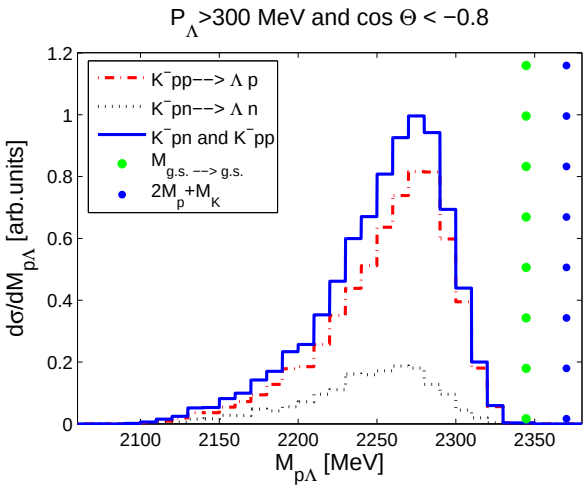

FIG. 5: (Color online) The same as Fig. 4, but imposing the experimental angle cut for back to back events, $\cos\Theta_{\vec{p}_\Lambda\vec{p}_p} < -0.8$.

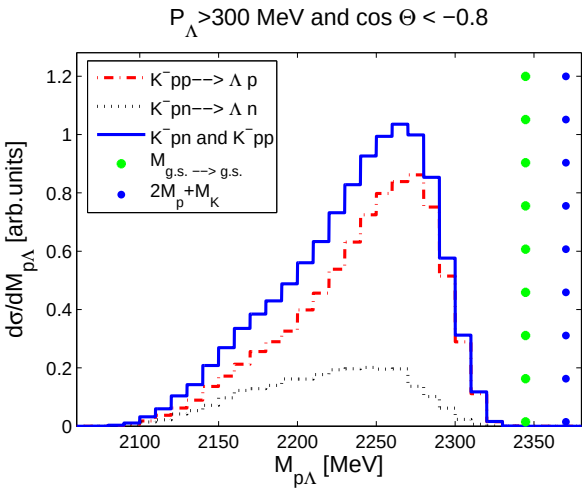

FIG. 7: (Color online) The same as Fig. 6, but imposing the experimental angle cut for back to back events, $\cos\Theta_{\vec{p}_\Lambda\vec{p}_p} < -0.8$.

followed by $np \to pn$ is represented in the figure by the dotted line. We can see that in the most interesting region, $\sqrt{s} = 2250 - 2300$ MeV, this process contributes only by about 20 % , while in the lower invariant mass region it becomes as important as the $K^-pp \to \Lambda p$ reaction. Low invariant masses correspond to the situation of Λp pairs with a low energy proton kicked above Fermi sea in a collision with the primary nucleon. We will see below that the amount of such events will increase when we allow more than one secondary collision.

Next we impose the remaining experimental restriction in our calculated spectrum, namely the back to back angle cut, $\cos\Theta_{\vec{p}_\Lambda\vec{p}_p} < -0.8$. This has a substantial effect, as can be seen in Fig. 5, narrowing considerably the invariant Λp mass spectrum, which looks now much more similar to the one in Fig. 3 of [34].

We can go further by allowing more collisions of the proton or Λ. In Fig. 6 and 7 we show, respectively, the spectrum of the Λp invariant mass without and with the experimental angle cut, and allowing up to three collisions of the Λ or p particles with the nucleons in the Fermi sea of the daughter nucleus. With respect to the one-collision case shown in Fig. 5, the spectrum of Fig. 7 shows a more clear peak at 2260 MeV, as in the insert of Fig. 3 in [34], and develops additional strength in the lower energy region, also present in the experimental data. The level of agreement of the prediction with the experimental data is the same as in other theoretical

studies of the quasielastic peak [40, 41, 42].

The angular distribution of the Λp events is shown in Fig. 8, where we have added to the spectrum with secondary collisions the calculated strength of the events corresponding to the g.s. to g.s. transition, which has been imposed to be about 10%. This fraction is about the one shown in Fig. 3 of Ref. [34] and roughly agrees with the magnitude estimated in previous section for ^{7}Li. A larger fraction than this would lead to an even more forward peaked distribution. However, as we discussed above, all the strength of these events is accumulated in a narrow peak of the Λp mass spectrum around the line of the light circles of Figs. 5,7 and has no influence on the broad peak of the spectrum. In our simulations, the g.s. to g.s. reaction corresponds to the case of no secondary collisions. We observe that the angular dependence of the peak for a transition to the g.s. of the daughter nucleus is obviously back to back, since the three particles participating in the absorption mechanism are practically at rest. Even assuming that the K^-pp system gets about 200 MeV/c momentum from the Fermi motion of the protons, this only leads to 4 MeV recoil energy for the daughter nucleus, making the Λp system move with velocity given as $\frac{200\ \mathrm{MeV}}{m_K+2M_p}$, and the angle between Λ and p fulfills $\cos\Theta_{\vec{p}_\Lambda\vec{p}_p} < -0.95$. Thus, all events of K^- absorption contributing to the narrow peak in the FINUDA experiment fall within the experimental cuts.

As we can see, the angular distribution of the total strength in Fig. 8 peaks back to back as in the experiment. We note that one should only expect a qualitative agreement with the angular distribution shown in Fig. 2 of [34], since that one is not corrected for the detector acceptance.

In order to explore the dependence of ours results on the atomic orbit assumed for the K^-, we show in Fig. 9 the calculated Λp invariant mass distribution for the K^- being absorbed in ^{12}C from a higher $3d$ orbit. It is clearly seen that the shape and centroid of the distribution are barely altered. Therefore, if the absorption of the K^- proceeds from an arbitrary superposition of the $2p$ and $3d$ orbits, the final spectrum would look just as those shown in Figs. 7 and 9.

In Figs. 10–13 we present the calculated Λp spectra for the other nuclei: ^{6}Li, ^{7}Li, ^{27}Al and ^{51}V. It is interesting to note that the width of the distribution gets broader with the size of the nucleus, while the peak remains in the same location, consistently to what one expects for the behavior of a quasielastic peak. We also observe that the spectra of heavy nuclei develop a secondary peak at lower invariant masses due to the larger amount of re-scattering processes as the particles move out of the nucleus. The spectrum presented in Fig. 3 of Ref. [34] collects data from the three lighter nuclei. However, to help clarifying the situation, it would be desirable to separate the contribution to the invariant mass spectra from the different nuclei, which might be done in the future. Let us note in this context that the work of [46] shows that the possible interpretation of the FINUDA peak as a bound state of

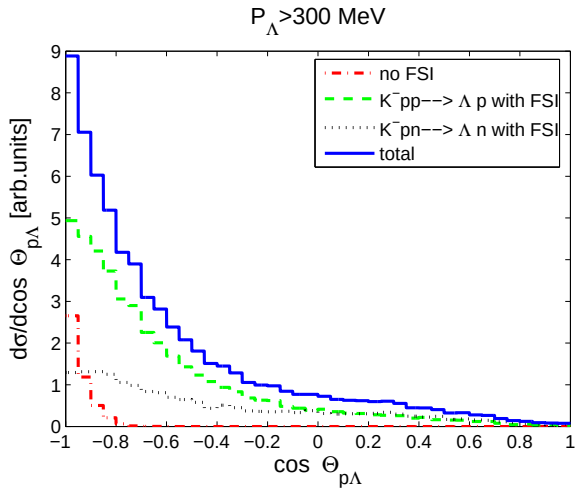

FIG. 8: (Color online) Opening angle distribution between a Λ and a proton in ^{12}C, allowing up to three collisions of the outgoing particles with the daughter nucleus. We assumed a 10% probability for the no FSI events, which correspond to those leaving the daughter nucleus in its ground state after K^- absorption.

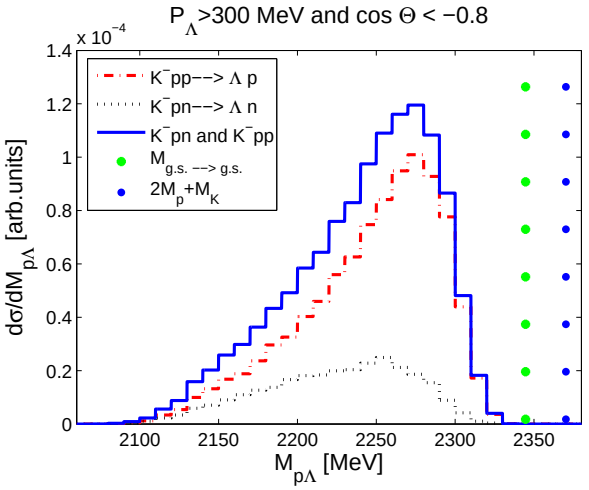

FIG. 9: (Color online) The same as Fig. 7, but assuming that K^- absorption proceeds from the atomic $3d$ orbit.

the K^- with the nucleus, not as a K^-pp bound state, would unavoidably lead to peaks at different energies for different nuclei.

Now we want to make a more quantitative comparison of our results with experimental data. We have combined our results for the first three light targets used in the FINUDA experiment in the same proportion as in the data [34] including kaon boost machine corrections [45], namely 51% ^{12}C, 35% ^{6}Li and 14% ^{7}Li. The proper absolute cross sections for the different nuclei (not those shown in the figures with arbitrary units for each nucleus) are taken into account for the weighted nuclear average.

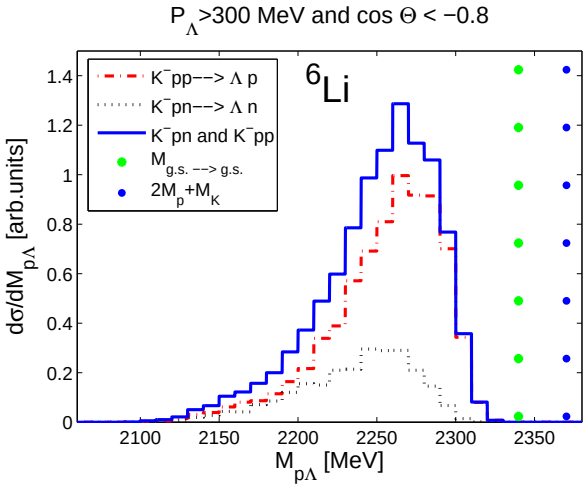

FIG. 10: (Color online) Invariant mass of Λp distribution for K^- absorption in ^{6}Li and allowing up to two collisions of the outgoing particles with the daughter nucleus.

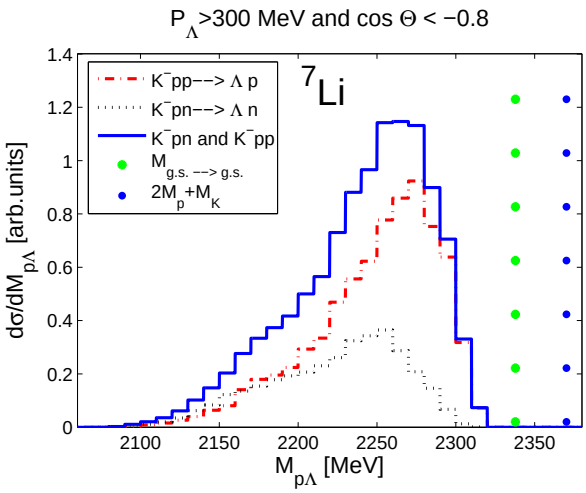

FIG. 11: (Color online) Invariant mass of Λp distribution for K^- absorption in ^{7}Li and allowing up to three collisions of the outgoing particles with the daughter nucleus.

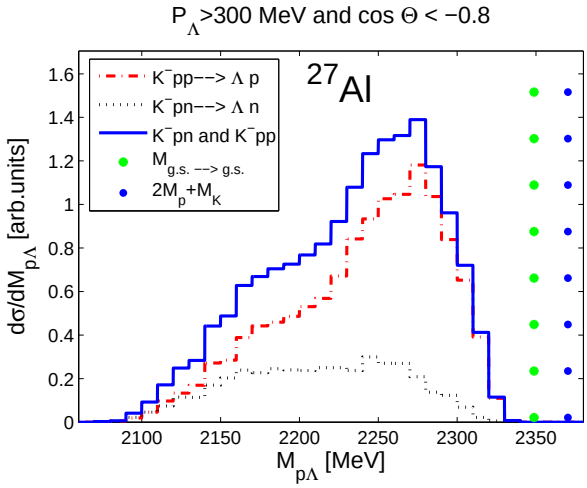

FIG. 12: (Color online) Invariant mass of Λp distribution for K^- absorption in ^{27}Al and allowing up to four collisions of the outgoing particles with the daughter nucleus.

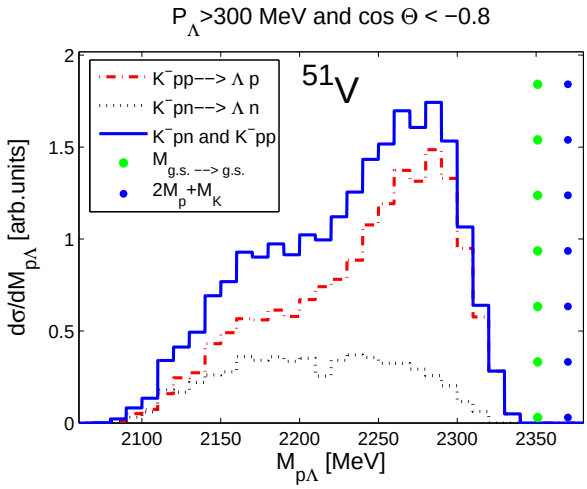

FIG. 13: (Color online) Invariant mass of Λp distribution for K^- absorption in ^{51}V and allowing up to five collisions of the outgoing particles with the daughter nucleus.

The final result, rescaled to the arbitrary units of [34], is shown versus experimental data with corresponding errorbars in Fig. 14 for the same energy range as in the insert of Fig. 3 in [34]. We can see that the agreement is very good, giving a χ^2 per data point of 1.25. It is important to mention here that our averaged histogram is dominated by the ^{12}C component of the mixture due, not only to the larger amount of protons and the higher probability of FSI in the bigger nucleus, but also, and mostly, to the larger overlap with the kaon wavefunction.

In summary, we have seen how the experimental spectrum is naturally explained in our Monte Carlo simulation as a consequence of final state interactions of the particles produced in nuclear K^- absorption as they leave the nucleus, without the need of resorting to exotic mechanisms like the formation of a K^-pp bound state.

V. FURTHER MECHANISMS

In this section, we explore other possible reactions which could also produce some strength in the region of energies addressed in the figures.

We start discussing the mechanism $K^-pp \to \Sigma^0 p$ followed by $\Sigma^0 \to \Lambda\gamma$, mentioned in [34] and discarded there with the claim "however, the observed invariant mass distribution is too broad to be attributed to this process only".

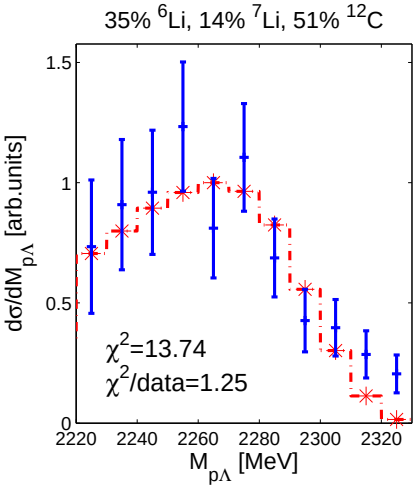

FIG. 14: (Color online) Invariant mass of Λp distribution for K^- absorption in light nuclei in the following proportion [34] including kaon boost machine corrections [45]: 51% ^{12}C, 35% ^{6}Li and 14% ^{7}Li. Stars and histogram show result of our calculations, experimental points and errorbars are taken from [34].

It is easy to check the kinematics by combining relativistically the momenta of the p from $K^-pp \to \Sigma^0 p$ and the Λ from $\Sigma^0 \to \Lambda\gamma$ and one obtains that the strength of this channel goes in the Λp invariant mass region between $\sqrt{s} = 2200$ MeV and $\sqrt{s} = 2265$ MeV and that all events fulfill the relative angle condition. With respect to the strength of this mechanism, we note that, according to the experimental findings of K^- absorption in ^{4}He [47], there is a fraction of 11.7 % for combined K^- absorption leading to $\Lambda(\Sigma^0)pnn$. This fraction is split into 2.3 % for Σ^0 and 9.4 % for Λ using arguments of isospin symmetry. Given the fact that isospin symmetry is badly broken at threshold [25], a different estimate was done in [24] providing a ratio of Λ to Σ^0 production of the order of one. For the estimates we assume an average between these two values, accepting large uncertainties, and we take $R = \Gamma(\Lambda p)/\Gamma(\Sigma^0 p) \approx 2$. Assuming now a fraction for the g.s. formation of the daughter nucleus similar for the two processes, there would be only about ~ 5 % of the K^- absorption width going to $\Sigma^0 p$ + g.s. followed by necessity by the $\Lambda\gamma$ (the main decay mode of the Σ^0). Therefore, even if the events fall within the relevant energy range, the strength of this mechanism is too small to have a significant effect in the main peak.

We consider now the K^- absorption events that go to $\Sigma^0 p$ followed by some collision of the p or Σ^0, with final $\Sigma^0 \to \Lambda\gamma$ decay as before. The fact that the Σ^0 and p have originally smaller momentum than the Λ and p in the $K^-pp \to \Lambda p$ absorption has as a consequence that fewer collisions overcome Pauli blocking and bigger collision angles are required to overcome it. This, together with the Λ momentum relative to the Σ^0, makes very small the fraction of events that fulfill the experimental condition $\cos\Theta_{\vec{p}_\Lambda \vec{p}_p} < -0.8$. A simple calculation shows that assuming $R = 2$, only a fraction of about 10 % of the big peak in Fig. 3 of [34] can come from this process, and these filtered events concentrate around $\sqrt{s} = 2250$ MeV.

Another source of Λp pairs to be investigated is the chain reaction $K^-NN \to \Sigma N_1$ followed by $\Sigma N_2 \to \Lambda p$, with N_2 a nucleon from the Fermi sea. We can have

$$\begin{aligned} K^-pp &\to \Sigma^+ n\,; \quad \Sigma^+ n \to \Lambda p \\ K^-pp &\to \Sigma^0 p\,; \quad \Sigma^0 p \to \Lambda p \\ K^-pn &\to \Sigma^0 n\,; \quad \Sigma^0 p \to \Lambda p \end{aligned} \tag{13}$$

According to [47] the combined rate for the three Σ formation reactions shown in the left column of Eq. (13) would be 3.3 % versus 9.9 % for Λp formation. If we take the ratio of Λ to Σ^0 production to be $R = 2$, as discussed earlier, the numbers would be 4.9 % versus 7.8 % . Therefore, roughly speaking, we can estimate the rate of ΣN formation as about one half of that of Λp. Next we demand that there is a collision with $\Sigma N \to \Lambda p$ conversion. The cross section for this reaction in the region of interest to us is of the order of 20 mb [48]. Using Eq. (11) with $\rho = \rho_0/2$, since in the second part of Eq. (13) the Λp conversion occurs only on neutrons or only on protons depending on the Σ charge, one obtains a survival probability of the order of 0.63 in ^{12}C and, correspondingly, a 37% probability for $\Sigma N \to \Lambda N$ conversion in the nucleus. All together, considering also the larger probability of NN or ΛN quasielastic collisions we find about one fourth of Λp events coming from this source compared to those from $K^-pp \to \Lambda p$ followed by Λ or p quasielastic collisions. However, when the Λ and p momenta in their c.m. frame are boosted to the rest frame of the nucleus where the Σ has about 450 MeV/c, the angle between the Λ and the p span a broad range and the fraction of events that fulfill the condition $\cos\Theta_{\vec{p}_\Lambda \vec{p}_p} < -0.8$ is very small. Together with the ratio one fourth of the events discussed above these contributions are negligible. That small fraction would peak in the region of $\sqrt{s} = 2170$ MeV, where indeed there is a little bump in Fig. 3 of [34].

One can also trace the, even fewer, events recombining the primary p from $K^-pp \to \Sigma^0 p$ with the Λ from $\Sigma N \to \Lambda N$ conversion. The same arguments also hold in this case and the angle cut constrain leaves a negligible amount of events from this mechanism to account for the spectrum of Fig. 3 of [34].

Note that we have concentrated only on two nucleon absorption events since these are the ones leading to highly back to back correlated Λp pairs. If one released this condition, other important one-body absorption mechanisms would contribute. For instance, considering the Fermi motion of the nucleons, the process $K^-N \to \Lambda\pi$ could produce a sizable fraction of Λ hyperons with momenta larger than 300 MeV/c, together with

a pion in the Δ resonance region. Further re-scattering of the Λ and the pion in the nucleus, or pion absorption, will produce relatively slow nucleons generating Λp events at lower invariant masses which are, however, uncorrelated in angle. Similar arguments hold for processes like $K^- N \to \Sigma\pi$ followed by $\Sigma N \to \Lambda N$ conversion in the nucleus.

The discussion on other possible sources of Λp pairs presented in this section reinforces our conclusions that the spectrum shown in Fig. 3 of [34] comes essentially from $K^- pN \to \Lambda N$ absorption followed by further interaction of the N or the Λ with other nucleons, with a small and narrow contribution coming from the formation of the g.s. of the daughter nucleus.

VI. CONCLUSIONS

In summary, we have seen that the Λp invariant mass distribution shown in Fig. 3 of [34] from K^- absorption in nuclei is naturally explained in terms of the $K^- pN \to \Lambda N$ reaction followed by further interaction of the N or the Λ in the daughter nucleus. The events with one collision account for the big peak in Fig. 3 of [34], interpreted there as a signal of the formation of the $K^- pp$ bound state. The bump at low invariant masses is accounted by events with two or more collisions. The small and narrow peak at higher invariant masses finds here the same interpretation as in [34], i.e. $K^- pp \to \Lambda p$ absorption leaving, however, the daughter nucleus in the ground state.

We have presented results for ^{6}Li, ^{7}Li, ^{12}C, ^{27}Al and ^{51}V, all of them measured by the FINUDA experiment, although the spectrum was only shown for the combined data of the three lighter nuclei. The width of the distribution increases with the nuclear mass while the peak stays in the same location, in accordance with our interpretation of it as coming from the quasielastic processes. Disentangling the spectrum for each of the nuclear targets used in the FINUDA experiment would be of particular relevance because a possible interpretation of the data as evidence of bound K^- nuclear states would unavoidably produce the peak at a different energy for each nucleus.

The explanation we have found has obvious experimental implications. Since the peak, claimed to be a signal for the $K^- pp$ bound state, is associated in our interpretation to the $K^- pN \to \Lambda N$ absorption followed by final state interactions of the N or the Λ with nucleons in the daughter nucleus, it should not appear if we produce the Λp pairs in elementary reactions. On the contrary, according to the interpretation of [34], if the $K^- pp$ system couples to Λp with such a large strength, so should the Λp system couple to the $K^- pp$ state at the Λp invariant mass given by the main peak in the insert of Fig. 3 of [34], $\sqrt{s} = 2260$ MeV. Such invariant masses are easily reachable in the $pp \to K^+ \Lambda p$ reaction at low energies. Although a devoted experiment for the present purpose has not been done, the present state of the art, with reactions like $pp \to K^+ p\pi^- X^+$ being currently considered [49], indicate that the $pp \to K^+ \Lambda p$ reaction is not particularly difficult, and its performance, looking at the Λp invariant mass, would be most instructive to further clarify the issue discussed here.

VII. ACKNOWLEDGMENTS

We would like to thank A. Gal for useful comments and for suggesting us to use a realistic antikaon atomic wave function. We also appreciate useful discussions with T. Bressani, P. Camerini, N. Grion and S. Piano. This work is partly supported by contracts BFM2003-00856 and FIS2005-03142 from MEC (Spain) and FEDER, the Generalitat de Catalunya contract 2005SGR-00343, and the E.U. EURIDICE network contract HPRN-CT-2002-00311. This research is part of the EU Integrated Infrastructure Initiative Hadron Physics Project under contract number RII3-CT-2004-506078.

[1] H. Toki and T. Yamazaki, Phys. Lett. B **213**, 129 (1988).
[2] H. Toki, S. Hirenzaki, T. Yamazaki and R. S. Hayano, Nucl. Phys. A **501**, 653 (1989).
[3] J. Nieves, E. Oset and C. Garcia-Recio, Nucl. Phys. A **554**, 509 (1993).
[4] E. Friedman and G. Soff, J. Phys. G **11**, L37 (1985).
[5] T. Yamazaki *et al.*, Z. Phys. A **355**, 219 (1996).
[6] K. Itahashi *et al.*, Phys. Rev. C **62**, 025202 (2000).
[7] H. Toki, S. Hirenzaki and T. Yamazaki, Nucl. Phys. A **530**, 679 (1991).
[8] S. Hirenzaki, H. Toki and T. Yamazaki, Phys. Rev. C **44**, 2472 (1991).
[9] C. J. Batty, E. Friedman and A. Gal, Phys. Rept. **287**, 385 (1997).
[10] E. Friedman and A. Gal, Phys. Lett. B **459**, 43 (1999).
[11] E. Friedman and A. Gal, Nucl. Phys. A **658**, 345 (1999).
[12] S. Hirenzaki, Y. Okumura, H. Toki, E. Oset and A. Ramos, Phys. Rev. C **61**, 055205 (2000).
[13] A. Baca, C. Garcia-Recio and J. Nieves, Nucl. Phys. A **673**, 335 (2000).
[14] V. Koch, Phys. Lett. B **337**, 7 (1994).
[15] M. Lutz, Phys. Lett. B **426**, 12 (1998).
[16] A. Ramos and E. Oset, Nucl. Phys. A **671**, 481 (2000).
[17] J. Schaffner-Bielich, V. Koch and M. Effenberger, Nucl. Phys. A **669**, 153 (2000).
[18] A. Cieply, E. Friedman, A. Gal and J. Mares, Nucl. Phys. A **696**, 173 (2001).
[19] Y. Akaishi and T. Yamazaki, Phys. Rev. C **65**, 044005 (2002).
[20] T. Suzuki *et al.*, Phys. Lett. B **597**, 263 (2004).

[21] Y. Akaishi, A. Dote and T. Yamazaki, Phys. Lett. B **613**, 140 (2005). [arXiv:nucl-th/0501040].

[22] M. Sato, talk at the Hadron Physics at COSY Workshop, Badhonnef (Germany), July 2005.

[23] M. Sato, talk at the PANIC05 Santa Fe Conference, October 2005.

[24] E. Oset and H. Toki, Phys. Rev. C, [arXiv:nucl-th/0509048].

[25] E. Oset and A. Ramos, Nucl. Phys. A **635**, 99 (1998).

[26] J. A. Oller and U. G. Meissner, Phys. Lett. B **500**, 263 (2001).

[27] D. Jido, J. A. Oller, E. Oset, A. Ramos and U. G. Meissner, Nucl. Phys. A **725**, 181 (2003).

[28] B. Borasoy, R. Nissler and W. Weise, Eur. Phys. J. A **25**, 79 (2005).

[29] J. A. Oller, J. Prades and M. Verbeni, Phys. Rev. Lett. **95**, 172502 (2005).

[30] T. Hyodo, S. I. Nam, D. Jido and A. Hosaka, Phys. Rev. C **68**, 018201 (2003).

[31] S. Prakhov *et al.* [Crystall Ball Collaboration], Phys. Rev. C **70**, 034605 (2004).

[32] V. K. Magas, E. Oset and A. Ramos, Phys. Rev. Lett. **95** (2005) 052301.

[33] M. Agnello *et al.* [FINUDA Collaboration], nucl-ex/0606021; A. Filippi *et al.* [FINUDA Collaboration], in Proceedings of Eleventh International Conference on Hadron Spectroscopy, Rio de Janeiro, Brazil, 21-26 August 2005, ed. A. Reis et al., AIP Conference Proceedings **814**, Melville, New York (2006). p. 598.

[34] M. Agnello *et al.* [FINUDA Collaboration], Phys. Rev. Lett. **94**, 212303 (2005).

[35] H.W. Baer, K.M. Crowe and P. Truol, Advances in Nuclear Physics, Ed. M. Baranger and E. Vogt, Vol 9, 1977, and references therein.

[36] M. Gmitro, H. R. Kissener, P. Truol, and R.A Eramzhyan, Sov. Jour. Part. and Nucl. **13**, 513 (1982); **14**, 323 (1983).

[37] F. Roig and J. Navarro, Nucl. Phys. A **440**, 659 (1985).

[38] H. C. Chiang, E. Oset, R. C. Carrasco, J. Nieves and J. Navarro, Nucl. Phys. A **510**, 573 (1990) [Erratum-ibid. A **514**, 749 (1990)].

[39] A. Ramos, E. Oset, L.L. Salcedo, Phys. Rev. C **50**, 2314 (1994).

[40] L. L. Salcedo, E. Oset, M. J. Vicente-Vacas and C. Garcia-Recio, Nucl. Phys. A **484**, 557 (1988).

[41] R. C. Carrasco, M. J. Vicente Vacas and E. Oset, Nucl. Phys. A **570**, 701 (1994).

[42] A. Gil, J. Nieves and E. Oset, Nucl. Phys. A **627**, 599 (1997).

[43] I. Vidaña, A. Polls, A. Ramos and H. J. Schulze, Phys. Rev. C **64**, 044301 (2001).

[44] M. Preston and R.K. Bhaduri, Structure of the Nucleus, Addison-Wesley, 1975.

[45] T. Bressani, private communication.

[46] J. Mares, E. Friedman and A. Gal, [arXiv:nucl-th/0601009].

[47] P. A. Katz, K. Bunnell, M. Derrick, T. Fields, L. G. Hyman and G. Keyes, Phys. Rev. D **1**, 1267 (1970).

[48] R. Engelman, H. Filthuth, V. Hepp and E. Kluge, Phys. Lett. **21**, 587 (1966); V. Hepp and M. Schleich, Z. Phys. **214**, 71 (1968); D. Stephen, Ph.D. Thesis, University of Massachusetts, 1970.

[49] I. Zychor *et al.*, Phys. Rev. Lett. **96**, 012002 (2006).